FINAL REPORT

(Project Reference: AOARD-06-4029)

Electron Impact Excitation Cross Sections of Xenon for Optical Plasma Diagnostic

Submitted to:

THE ASIAN OFFICE

OF AREOSPACE RESEARCH & DEVELOPMENT

Submitted by:

Dr. Rajesh Srivastava, Professor

Department of Physics

Indian institute of Technology (I.I.T.)

Roorkee-247667

INDIA

Report Documentation Page

Form Approved
OMB No. 0704-0188

1. REPORT DATE	2. REPORT TYPE	3. DATES COVERED
20 NOV 2007	**Final**	**25-04-2007 to 27-06-2007**

4. TITLE AND SUBTITLE
Electron Impact Excitation Cross Sections of Xenon for Optical Plasma Diagnostics

5a. CONTRACT NUMBER
FA48690610044

5b. GRANT NUMBER

5c. PROGRAM ELEMENT NUMBER

6. AUTHOR(S)
Rajesh Srivastava

5d. PROJECT NUMBER

5e. TASK NUMBER

5f. WORK UNIT NUMBER

7. PERFORMING ORGANIZATION NAME(S) AND ADDRESS(ES)
Indian Institute of Technology, Roorkee,IIT Roorkee,Roorkee ,India,IN,247667

8. PERFORMING ORGANIZATION REPORT NUMBER
N/A

9. SPONSORING/MONITORING AGENCY NAME(S) AND ADDRESS(ES)
AOARD, UNIT 45002, APO, AP, 96337-5002

10. SPONSOR/MONITOR'S ACRONYM(S)
AOARD-064029

11. SPONSOR/MONITOR'S REPORT NUMBER(S)

12. DISTRIBUTION/AVAILABILITY STATEMENT
Approved for public release; distribution unlimited

13. SUPPLEMENTARY NOTES

14. ABSTRACT
In this project the researcher had taken up the calculation of xenon apparent emission-excitation cross sections for emission lines that have diagnostic value in the analysis of Xe-propelled electric thruster plasmas. Following conclusions were made from the study ï¿½The RDW method has been shown to be applicable to transitions between excited states. ï¿½Since the excitation energy of these transitions is relatively small, first-order theories are valid at lower energies than for excitations from the ground states. ï¿½The accuracy of the cross section depends crucially on the accuracy of the oscillator strengths obtained from the target wave functions. ï¿½The use of a relativistic formalism (j-j coupling) clearly explains the huge variation in the magnitudes of these cross sections. ï¿½The objectives of the project have been achieved and the aimed metastable excitation cross section results of xenon were obtained that are required for the CRM model of Dressler and co workers and these are being tested and new plasma modeling results are under calculation.

15. SUBJECT TERMS

16. SECURITY CLASSIFICATION OF:			17. LIMITATION OF ABSTRACT	18. NUMBER OF PAGES	19a. NAME OF RESPONSIBLE PERSON
a. REPORT	b. ABSTRACT	c. THIS PAGE			
unclassified	**unclassified**	**unclassified**	**Same as Report (SAR)**	**20**	

Outline of the Report

1. Introduction and Background of the Project

In this project we had proposed to take up the calculation of xenon apparent emission-excitation cross sections for emission lines that have diagnostic value in the analysis of Xe-propelled electric thruster plasmas. In fact, these cross sections are vital for models that are necessary for proper integration and lifetime predictions of Hall effect thrusters. The experimental measurement of cross section and plasma related analysis in this connection have been in progress and are being carried out by Dr. R. A. Dressler and his group at the Air Force Research Laboratory, Hanscom AFB [1]. To supplement this work we had planned to perform at I.I.T. Roorkee in India reliable calculations for electron impact excitation cross section to provide relevant cross section data needed for the study of xenon propelled electric thrusters. Below we briefly introduce the xenon propelled electric thrusters.

An ion engine relies on electrically charged atoms, or ions, to generate thrust. Xenon, an inert, noncombustible gas, is electrically charged and the ions are accelerated to a speed of about 62,900 miles per hour (30 kilometers per second). The ions are then emitted as exhaust from the thruster (see figure below of an ion engine for illustration), creating a force, which propels the spacecraft in the opposite direction. The primary advantage of electric propulsion is efficiency. An ion engine is 10 times more efficient than its alternative, a chemical propulsion system. With xenon, it is possible to reduce propellant mass onboard a spacecraft by up to 90 percent. The advantages of having less onboard propellant include a lighter spacecraft, and, since launch costs are set based on spacecraft weight, reduced launch cost.

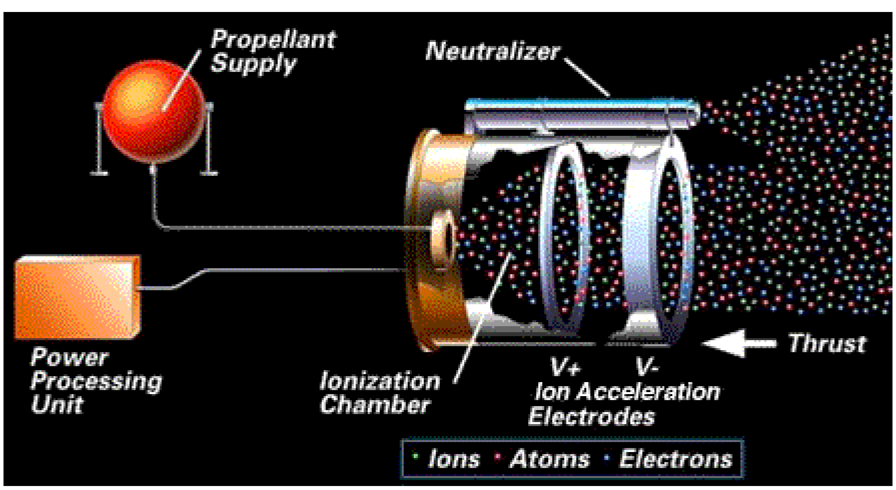

The use of these electrostatic thrusters, however, poses new challenges regarding their proper engineering and integration on satellites. Precise modeling of the satellite plasma environment is required. A suitable approach is required for analyzing xenon-propelled Hall thruster optical radiation based on apparent electron and ion impact emission cross sections associated with lines in visible and near-infrared region of the spectrum.

The current proposal addresses as a first step to get accurate theoretical electron impact cross sections for the processes where initially excited metastable states viz. $1s_3$ and $1s_5$ of xenon are excited by electrons to the $2p_n$ states with n =1,10 in Paschen's notation. For these excitations no other theoretical calculations are available and also scarce experimental data have been reported [2,3].

We address here in this project the Hall effect thrusters (HET), which are a high-specific impulse alternative to chemical propulsion systems of spacecraft [1,4]. In HETs, a gas, typically xenon or krypton, is efficiently ionized in a discharge, and positive ions are electrostatically accelerated to generate thrust. The performance, plasma characteristics, and durability of HETs are extensively evaluated both in ground-based test facilities and in space. Basic characteristics of HET plasmas, such as charge species densities and temperatures have been traditionally measured by various plasma probes. However, at HET conditions, traditional plasma-probe diagnostics are affected by problems such as the perturbation of the local environment by the probe, the complexity associated with interpreting the probe characteristics, and detrimental effects in regions of high temperatures (e.g., in the HET discharge). Consequently, HET plasma parameters reported from probe experiments exhibit significant disparities. Optical plasma diagnostics circumvent these problems and are thus an attractive alternative to probe measurements.

A key component of collisional radiative model (CRM) is a set of emission cross sections associated with the energy transfer processes that lead to population of states that radiatively relax through emission in the spectral region of interest [1,4]. Proper implementation of a CRM has been primarily hampered by the lack of a comprehensive cross section set. In fact, these cross sections are vital for models that are necessary for proper integration and lifetime predictions of Hall effect thrusters (HET). If we focus on emission excitation cross sections for Xe propelled HETs, the optical radiation arises from electron – xenon atom collisions, of which

the most important contribution can be assumed to be coming from following excitation processes:

$$e^{-} + Xe \rightarrow Xe^{*} + e^{-} \tag{1}$$

$$e^{-} + Xe^{m} \rightarrow Xe^{*} + e^{-} \tag{2}$$

The asterisks in processes (1) and (2) signify excited species that lead to optical emissions. Superscript *m* indicates metastable states. The process (1), which deals with the excitation of xenon from the ground state to upper excited states have been studied theoretically and experimentally [1-4]. The process (2) which deals with excitation of the metastable state has not been explored.

Metastable states of the noble gases are important constituents of plasmas. In addition to their long lifetime, these states have large inelastic cross sections as compared to the excitation from the ground state [3]. Thus it is important to include these processes in the modeling of plasma which is prime objective of the present project.

2. Outline of the work done

- Electron impact excitation of xenon atoms from metastable states to upper $2p_n$ (n = 1-10) excited states have been considered.
- Excitation cross sections are calculated using the Relativistic distorted-wave (RDW) theory.
- Fine-structure atomic states are represented by multi- configuration Dirac-Fock wave functions.
- Continuum projectile electron distorted waves are obtained through Dirac equations.
- Calculations are compared with experimental results [2].
- The cross sections are incorporated in the CRM model i.e. in the analysis of Xe-propelled electric thruster plasmas, being carried out by Dr. R. Dressler at AFB, Hanscom [1,4].

3. Detailed Description of the Work done

3.1 Energy levels of Xenon

- The ground state of xenon has $5p^6$ configuration.
- The first excited state has a $5p^5 6s$ configuration with four fine-structure levels with $J = 0, 1, 1, 2$.
- The states with $J = 0$ and 2 are long-lived metastable states i.e. $1s_3$ and $1s_5$ states.
- We consider the electron excitation of these two metastable states to the higher lying $5p^5 6p$ configuration having ten fine-structure levels i.e. $2p_n$ (n = 1-10) excited states.

The figure below shows the energy levels of the xenon

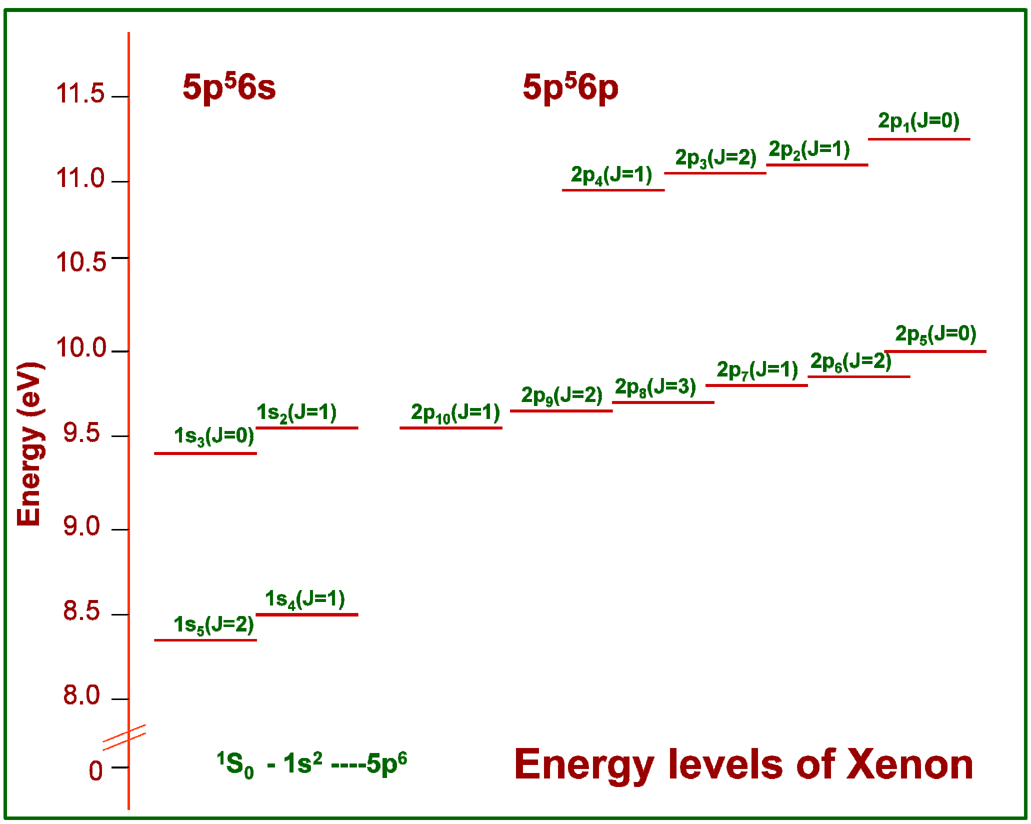

3.2 Description of the states in relativistic j-j coupling scheme

The ground states of the noble gases have an np^6 outer shell in the nonrelativistic representation where n = 5 for xenon.

In the relativistic *j-j* coupling scheme, this shell is broken into two subshells and represented as n$\overline{p}^2$np^4 where $\overline{p}$ represents a p electron with total angular momentum (orbital angular momentum plus spin) j = 1/2 while p has j = 3/2.

Thus the metastable states have configurations

		Paschen notation
$5\overline{p}^2 5p^3 6s$	with J=2	$1s_5$
$5\overline{p} 5p^4 6s$	with J=0	$1s_3$

Upper states have configurations

$5\overline{p}^2 5p^3 6p$	with J = 0, 1, 2, 3
$5\overline{p}^2 5p^3 6\overline{p}$	with J = 1, 2
$5\overline{p} 5p^4 6p$	with J = 1, 2
$5\overline{p} 5p^4 6\overline{p}$	with J = 0, 1

These upper ten states are represented in the Paschen notation by $2p_1$ - $2p_{10}$ in order of decreasing energy but order of J values may change with atom. The following figure shows diagrammatically the excitation transitions considered in the present work.

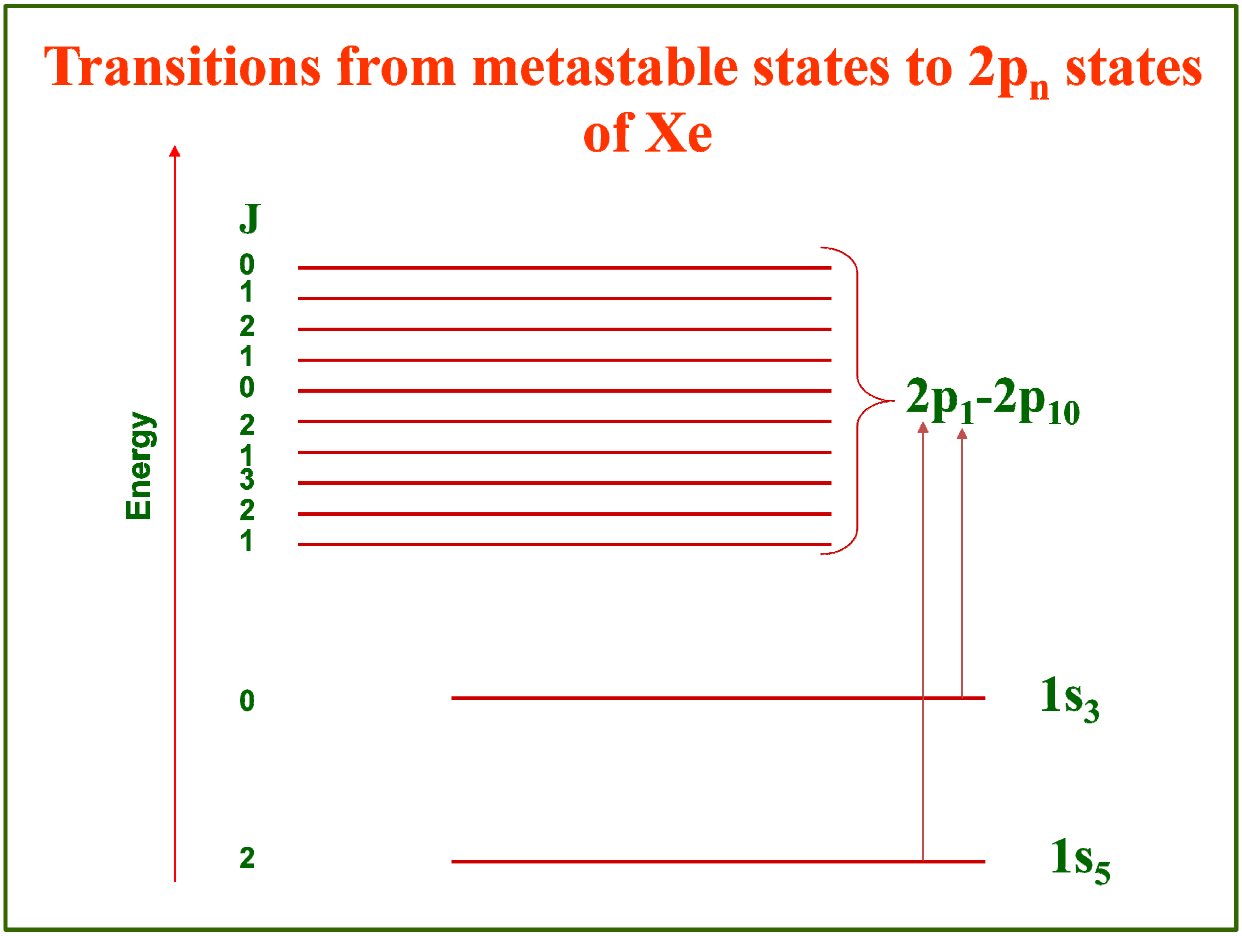

4. Calculation of Excitation Cross Sections in Xenon

For cross section calculation we use relativistic distorted wave (RDW) method. The salient features of the RDW are as follows:

4.1 Salient features of RDW method

- As relativistic effects should be included in the study of electron impact excitation of heavy atoms where spin-orbit effects are important, our method incorporates full relativistic effects.
- Our method considers directly the fine-structure target states without any approximation.
- Our method includes spin-polarized electrons in a natural way.

- Our Relativistic Distorted Wave (RDW) method involves solving the Dirac equations to describe both the bound and continuum electrons.
- The relativistic effects are thus incorporated to all orders in a natural way.

4.2 Brief Description of RDW Theory

The distorted-wave T-matrix for the electron impact excitation of an atom having N electrons and nuclear charge Z from an initial state i to final state f can be written as (atomic units are used throughout)

$$T_{i\to f}^{DW} = \left\langle \chi_f^-(1,\ 2,\ .....,\ N+1)\middle| V - U_f(N+1) \middle| A\chi_i^+(1,\ 2,\ .....,\ N+1)\right\rangle$$

where V is the target-projectile interaction given by

$$\mathrm{V} = -\frac{\mathrm{Z}}{\mathrm{r_{N+1}}} + \sum_{\mathrm{j=1}}^{\mathrm{N}} \frac{1}{\left|\mathbf{r_j} - \mathbf{r_{N+1}}\right|}$$

here

$\mathbf{r}_j$ (j = 1, …, N)	position co-ordinates of the target electrons
$\mathbf{r}_{N+1}$	position co-ordinate of the projectile electron with respect to the nucleus of the atom
U_f	distortion potential
A	antisymmetrization operator

<u>The wave functions $\chi_{ch}^{+(-)}$</u>, where 'ch' refers to the two channels, i.e. initial 'i' and final 'f', are represented as a product of the <u>N-electron target wave functions ϕ_{ch}</u> and <u>a projectile-electron distorted-wave function</u> $\mathrm{F_{i(f)}^{DW+(-)}}$,i.e.

$$\chi_{\mathrm{ch}}^{+(-)}(1,\ 2,\ .....,\ \mathrm{N}+1) = \phi_{\mathrm{ch}}(1,\ 2,\ .....,\ \mathrm{N})\ \mathrm{F_{ch}^{DW+(-)}}(\mathbf{k}_{\mathbf{ch}}, \mathrm{N}+1).$$

Here '+' refers to an outgoing wave while '-' denotes an incoming wave.

<u>The projectile electron continuum wavefunctions</u> are given by

$$\mathrm{F}_{\mu}^{\pm}(\mathbf{k},\mathbf{r}) = \frac{1}{(2\pi)^{3/2}} \sum_{\kappa m} \mathrm{e}^{\pm i\eta_\kappa}\, \mathrm{a}_{\kappa m}^{\mu}(\hat{k}) \frac{1}{r} \begin{pmatrix} f_\kappa(r)\ \chi_{\kappa m}(\hat{r}) \\ i g_\kappa(r)\ \chi_{-\kappa m}(\hat{r}) \end{pmatrix}$$

where

$$\mathrm{a}_{\kappa m}^{\mu}(\hat{k}) = 4\pi i^l \left[\frac{E+c^2}{2E}\right]^{1/2} \sum_{m_l} (l\ m_l\ \tfrac{1}{2}\ \mu |\ j\ m) Y_{l\,m_l}^{*}(\hat{k})$$

μ magnetic component of spin of projectile electron

$\mathbf{k}_{ch}$ wave vector of the projectile electron in the initial and final state

f larger component of the radial part of the wavefunction

g smaller component of the radial part of the wavefunction

η phase shift

E relativistic energy of the incident electron

The spin-orbit functions are given by

$$\chi_{\kappa m}(\hat{\mathbf{r}},\sigma)=\sum_{\mu\nu}(\ell\,\mu\,\tfrac{1}{2}\nu|\;j\,m)Y_{\ell\,\mu}(\hat{\mathbf{r}})\psi_{\frac{1}{2}\nu}(\sigma)$$

and

$$\chi_{-\kappa m}(\hat{\mathbf{r}},\sigma)=\sum_{\mu\nu}(\tilde{\ell}\,\mu\tfrac{1}{2}\nu|\;j\,m)Y_{\tilde{\ell}\,\mu}(\hat{r})\psi_{\frac{1}{2}\nu}(\sigma)$$

where

J total angular momentum of the orbital

m the z-component of j

$\psi_{(1/2)\nu}(\sigma)$ normalized two-component spin wave functions

and $\tilde{\ell}=2j-\ell$

The spin-angular state is characterized by quantum number κ, which is defined as

$$\kappa = \begin{cases} \ell & if \quad j=\ell\text{-}1/2 \quad \text{for } \ell>0 \\ -\ell-1 & if \quad j=\ell+1/2 \end{cases}$$

The radial parts $f_\kappa(r)$ and $g_\kappa(r)$ are obtained from the Dirac equations

$$\left(\frac{d}{dr}+\frac{\kappa}{r}\right)f_\kappa(r)-\frac{1}{c}(c^2-U+E_{ch})g_\kappa(r)-\frac{1}{cr}W_Q(\kappa;r)=0$$

$$\left(\frac{d}{dr}-\frac{\kappa}{r}\right)g_\kappa(r)+\frac{1}{c}(-c^2-U+E_{ch})f_\kappa(r)+\frac{1}{cr}W_P(\kappa;r)=0$$

Here U is distortion potential and W is exchange terms

Dirac equations are solved using the boundary conditions

$$f_\kappa(r)\xrightarrow[r\to\infty]{}\frac{1}{k}\sin(k_{ch}r-\frac{l\pi}{2}+\eta_\kappa)$$

$$g_\kappa(r)\xrightarrow[r\to\infty]{}\frac{c}{c^2+E_{ch}}\cos(k_{ch}r-\frac{l\pi}{2}+\eta_\kappa)$$

Wave function $\Phi_{a(b)}$ of the target atom is solution of Dirac equation with Hamiltonian

$$H_{atom} = \sum_{j=1}^{N}\left[-ic\alpha\nabla_j + \beta c^2 - \frac{Z}{r_j}\right] + \sum_{i<j}^{N}\frac{1}{\left|\mathbf{r}_i - \mathbf{r}_j\right|}$$

The single electron central field Dirac orbitals are given by

$$\Phi_{n\kappa m}(\mathbf{r},\sigma)=\frac{1}{r}\begin{pmatrix} P_{n\kappa}(r)\,\chi_{\kappa m}(\hat{\mathbf{r}},\sigma) \\ iQ_{n\kappa}(r)\,\chi_{-\kappa m}(\hat{\mathbf{r}},\sigma)\end{pmatrix}$$

where

α, β Dirac matrices
$i\boldsymbol{\nabla}_j$ momentum operator of the jth target electron
$P_{n\kappa}$ larger component of the radial part of the wavefunction
$Q_{n\kappa}$ smaller component of the radial part of the wavefunction

The bound state orbitals satisfy the following orthogonality conditions,

$$\int_0^\infty dr\left[P_{n'\kappa}(r)P_{n\kappa}(r)+Q_{n'\kappa}(r)Q_{n\kappa}(r)\right]=\delta_{n'n}$$

$$\left\langle \chi_{\kappa m}(\hat{r},\sigma)\middle|\chi_{\kappa' m'}(\hat{r},\sigma)\right\rangle = \delta_{\kappa'\kappa}\,\delta_{m'm}$$

After obtaining the wavefunctions for target atom bound states and the projectile electron continuum states, We evaluate the scattering amplitude for the excitation of a noble gas atom in a metastable state with total angular momentum J_{i} and magnetic quantum number M_{i} to a final $5p^5 6p$ state with angular momentum J_{f}, M_{f} as

$$f(J_f,M_f,\mu_f;J_i,M_i,\mu_i)=(2\pi)^2\sqrt{\frac{k_f}{k_i}}T^{DW}_{i\to f}(J_f,M_f,\mu_f;J_i,M_i,\mu_i)$$

where μ_i and μ_f are the spin projections in the initial and final channels. Then with our normalization the differential cross section (DCS) is given by

$$DCS=\frac{1}{2(2J_i+1)}\sum_{M_i,\mu_i,M_f,\mu_f}\left|f(J_f,M_f,\mu_f;J_i,M_i,\mu_i)\right|^2$$

and the ICS is obtained by integrating the DCS over all scattering angles.

$$\sigma_{Tot} = \int\frac{d\sigma}{d\Omega}d\Omega$$

4.3 Calculation of the Atomic wave functions

The metastable states are single configuration wave functions.

$$\Phi_{J=2} = 5\overline{p}^2 5p^3 6s$$

$$\Phi_{J=0} = 5\overline{p} 5p^4 6s$$

The excited $2p_n$ states are linear combinations of the $5p^5 6p$ configurations with the same *J* value.

$$\Phi_J = c_1 5\overline{p}^2 5p^3 6\overline{p} + c_2 5\overline{p}^2 5p^3 6p + c_3 5\overline{p} 5p^4 6\overline{p} + c_4 5\overline{p} 5p^4 6p$$

The mixing coefficients c_i's of the various configurations to the fine-structure levels of the final states are given in tables 1. These wave functions are Dirac-Fock wave functions calculated from the GRASP92. To optimize the wavefunctions obtained, we have compared in table 2, our calculated values of energy differences with the corresponding experimental values listed in NIST Database [5]. We have also presented in table 3 the comparison of our calculated optical oscillator strengths with the available theoretical [6] and experimental [2] results for the optically allowed transitions.

Table 1. Contributions of the various configurations to the $5p^5 6p$ states of Xe

Configurations	$5\overline{p}^2 5p^3 6\overline{p}$	$5\overline{p}^2 5p^3 6p$	$5\overline{p} 5p^4 6\overline{p}$	$5\overline{p} 5p^4 6p$
J = 0 levels				
$2p_1$		0.0009	0.9991	
$2p_5$		0.9991	0.0009	
J = 1 levels				
$2p_2$	0.0045	0.0027	0.0040	0.9878
$2p_4$	0.0001	0.0019	0.9937	0.0043
$2p_7$	0.4306	0.5679	0.0015	10^{-7}
$2p_{10}$	0.5649	0.4264	0.0008	0.0079
J = 2 levels				
$2p_3$	0.0006	0.0004		0.9990
$2p_6$	0.0527	0.9467		0.0006
$2p_9$	0.9467	0.0529		0.0004

Table 2. Energy differences (eV) for the transitions considered: NIST - experimental values from the NIST database [5]; GRASP - calculated values using the GRASP92 program

Transition	NIST	GRASP
1*s*5- 2*p*10	1.26483	1.01583
1*s*5 - 2*p*9	1.3703	1.11376
1*s*5 - 2*p*8	1.40542	1.13561
1*s*5 - 2*p*7	1.47398	1.21215
1*s*5 - 2*p*6	1.50577	1.23393
1*s*5 - 2*p*5	1.61816	1.30729
1*s*5 - 2*p*4	2.64229	2.44226
1*s*5 - 2*p*3	2.7394	2.50259
1*s*5 - 2*p*2	2.75383	2.49999
1*s*5 - 2*p*1	2.8259	2.56711
1*s*5- 1*s*3	1.13187	1.3239

Table 3: Dipole oscillator strengths for transitions in Xe: GRASP92, present calculations; Theory, theoretical calculations [6]; Expt., values derived from high energy cross section measurements [2].

Initial state		$1s_5$		$1s_3$	
Final state	GRASP	Theory	Expt	GRASP	Theory
$2p_{10}$	0.200	0.268		0.00021	0.0249
$2p_9$	0.112	0.132			
$2p_8$	0.571	0.641	0.59±0.19		
$2p_7$	0.0227	0.0117		3.09×10^{-5}	0.00496
$2p_6$	0.321	0.253	0.30±0.10		
$2p_4$	6.09×10^{-5}	7.67×10^{-4}		0.482	0.286
$2p_3$	0.0009	0.00266			
$2p_2$	0.004	6.55×10^{-4}		0.760	0.382

5. Xenon Cross Sections: Results, Discussion and Conclusion

We observe that the transitions we considered are of the following type

- Transitions from the $1s_5$ $J = 2$ state are allowed to the $2p_n$ states with $J = 1, 2, 3$.
- Transitions from the $1s_3$ $J = 0$ state are allowed only to the $2p_n$ states with $J = 1$.

- All other transitions are forbidden but the transition from $1s_3$ $J = 0$ state to the $2p_n$ states with $J = 3$ is identically zero in a first-order theory.

The figure below shows diagrammatically the all optically allowed transitions from metastable states to $2p_n$ states of Xe

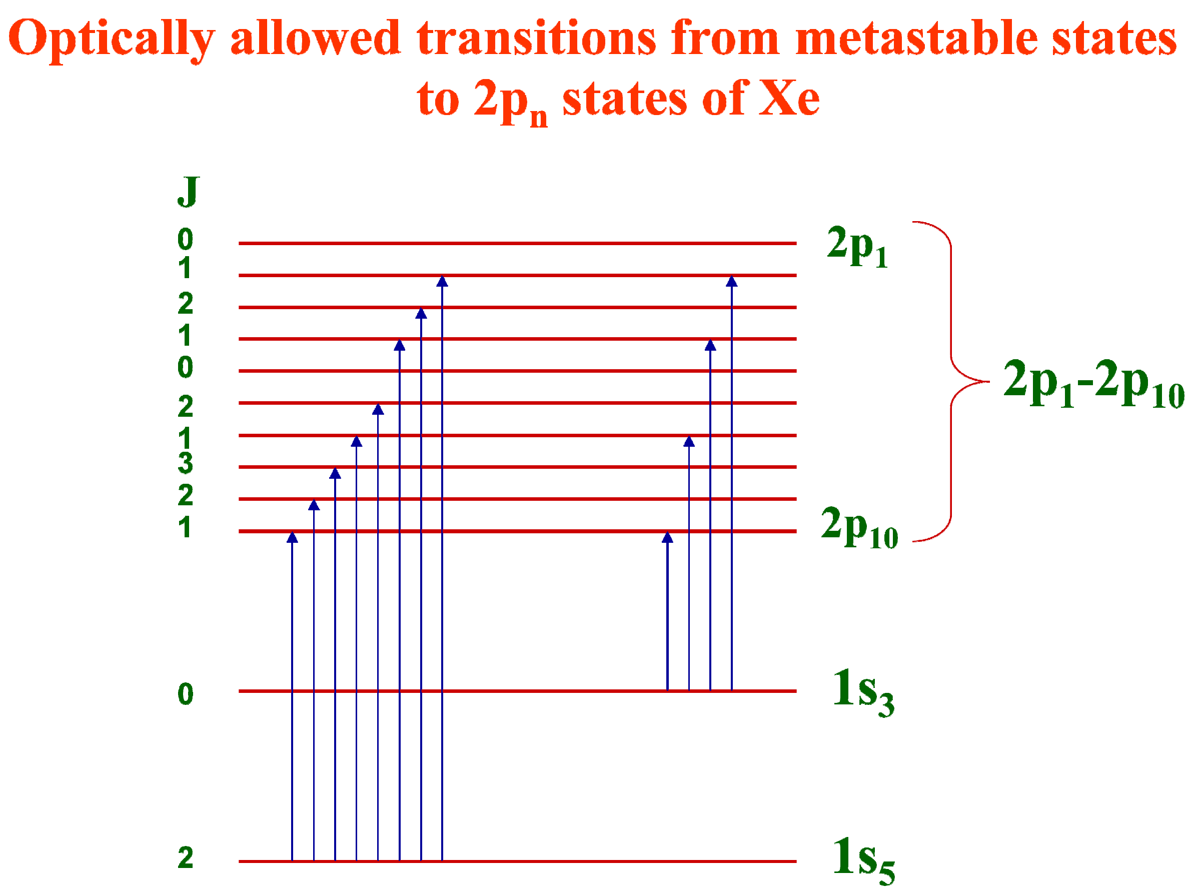

Fitting of the calculated allowed transition cross sections:

For allowed transitions we find the cross section takes on the Bethe-Born form at larger energies

$$\sigma = 4\pi a_0^2 \frac{f}{E\Delta E}[\ln(E)+b]$$

where

E energy of the incident electron in Rydbergs
ΔE excitation energy of the transition
f optical oscillator strength of the transition
b fitting constant

We have fitted our excitation cross section results to the above Bethe-Born formula and the fitting constant ‘b’ for the allowed transitions is given in table-4.

Table 4: Values of constant b for allowed transitions

Atom	Xenon	
Initial State	$1s_3$	$1s_5$
Final State		
$2p_{10}$	43.6192	2.8511
$2p_9$	-	2.7067
$2p_8$	-	2.6077
$2p_7$	12.9306	2.5839
$2p_6$	-	2.3348
$2p_5$	-	-
$2p_4$	2.4934	1.3368
$2p_3$	-	1.2852
$2p_2$	2.3252	1.2952
$2p_1$	-	-

These fitted cross sections, thus, allow us to predict the cross section at any desired energy and can be easily used in plasma modeling as such.

At larger energies we find that the cross sections for forbidden transitions behave as E^{-3} where E is the energy of the incident electron.

Comparison of our cross sections with available experimental results

Jung *et al* [2] have recently published measurements of cross sections for the excitation from the metastable $1s_5$ state of Xe to the $\{2p_5 - 2p_{10}\}$ manifold. Only two of these transitions ($2p_6$ and $2p_8$) were measured at higher energies. For excitation to the $J = 1$ states, which are allowed transitions from either of the metastable initial states, those that involve a change of core configurations are several orders of magnitude smaller than those that don’t. We note that the cross section for the $1s_5$ - $2p_7$ transition is much smaller than for the others without a change in core which is in conformity with the magnitudes of the oscillator strengths.

We compare our results with the measured cross sections of Jung *et al* [2] in Figures 1 and 2. Our cross sections agree reasonably well with the measured cross sections at larger energies for the excitation of the $2p_6$ and $2p_8$ states but there is a systematic deviation as the incident electron energy decreases being roughly a factor of two larger around 8 eV. The agreement with those transitions which were not measured at higher energies is comparable to

these two cases. Our cross sections are always above the measured values at 8 eV with the exception of that for the $2p_5$ state which may imply that cascade contributions from more highly excited states are larger in this case as suggested by Jung *et al* [2].

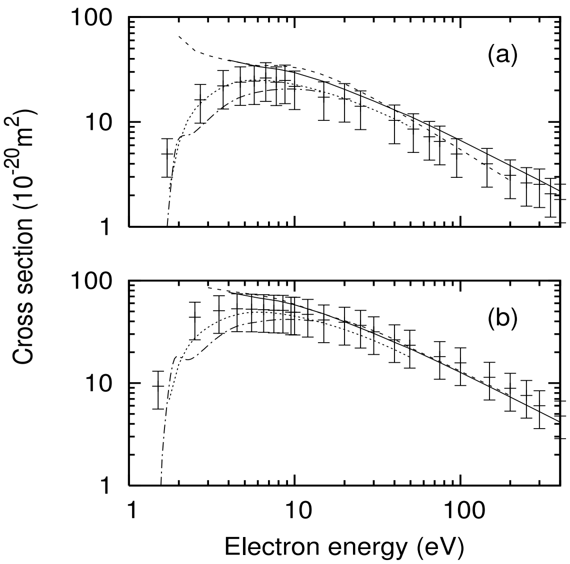

Figure 1: Integrated cross sections for electron excitation of xenon from the $1s_5$ state to the: (a) $2p_6$ state; (b) $2p_8$ state. Solid curve, presents RDW calculations; experimental points with error bars, Jung *et al* [2].

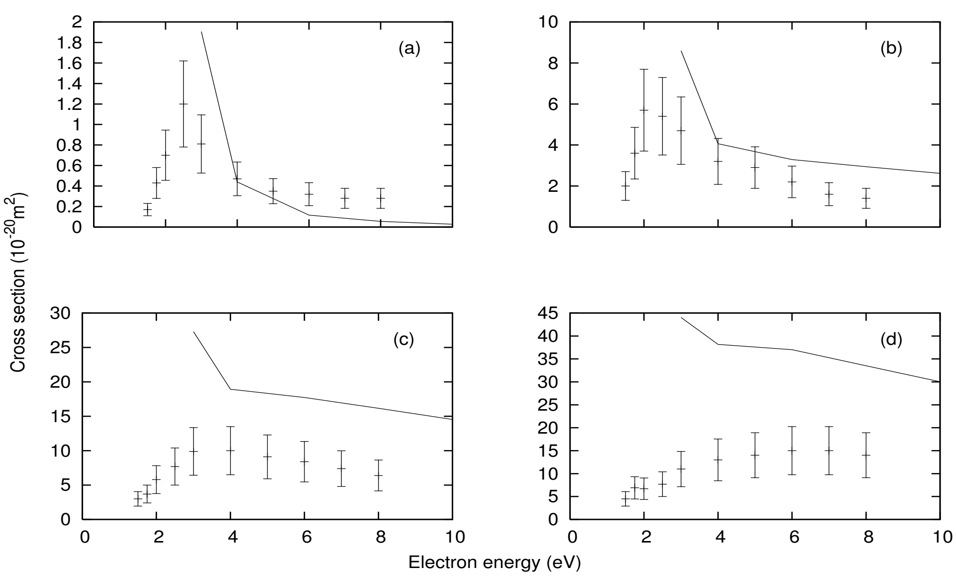

Figure 2: Integrated cross sections for electron excitation of xenon from the $1s_5$ state to the: (a) $2p_5$ state; (b) $2p_7$ state; (c) $2p_9$ state; (d) $2p_{10}$ state. Solid curve, presents RDW calculations; experimental points with error bars, Jung *et al* [2].

The following conclusions can be drawn from the above presentation of our results

- The RDW method has been shown to be applicable to transitions between excited states.
- Since the excitation energy of these transitions is relatively small, first-order theories are valid at lower energies than for excitations from the ground states.
- The accuracy of the cross section depends crucially on the accuracy of the oscillator strengths obtained from the target wave functions.
- The use of a relativistic formalism (*j-j* coupling) clearly explains the huge variation in the magnitudes of these cross sections.
- We have presented here our selected results and these are now published [7] and presented at various conferences (see the section of list of publications).
- Our entire results published and unpublished will be utilized in the future modeling calculations.
- We have achieved our target and obtained the aimed metastable excitation cross section results of xenon required for the CRM model of Dressler and co workers [1,4] and these are being tested and new plasma modeling results are under calculation.

6. Application of Cross sections to CRM Model of Dressler and co workers

We have been informed that our calculations of electron-excitation from the $5p^5 6s$ J=2 metastable level ($1s_5$ state in Paschen notation) to the lowest six $5p^5 6p$ ($2p$) levels have allowed Dressler and co workers at AFB Hanscom to develop a collisional radiative model (CRM) for Xe near-infrared (NIR) emissions based on population and depopulation of the metastable level through $1s_5 - 2p$ transitions. Application of the model to spectral intensities observed in the plume of a Hall thruster, however, demonstrates that the model overestimates the population of the $1s_5$ state. The observed spectrum can be reproduced with high fidelity if additional metastable de-excitation mechanisms are effective.

On the demand of the Hanscom Group, we have further carried out calculations for the excitation of xenon from its $1s_5$ level to $1s_2$, $1s_3$ and $1s_4$ levels. Thereafter, the group has demonstrated that the electron-induced depopulation through the excitation to $5p^5 6s$ J=1 ($1s_4$) and other $5p^5 6s$ levels, for which newly calculated cross sections are presented, can account for the additional de-

excitation mechanisms and give reliable results. This work we are planning to present in the GEC-2007 meeting to be held at Arlington VA, during October 2 -5, 2007 (see list of publications).

7. Future Work

In the light of recent experimental results of Jung et al [8] we have carried out relativistic distorted wave calculations for electron impact excitation of the ten higher-lying fine-structure levels of the $3p^5 5p$ configuration of argon from the lowest metastable states (the $J = 0, 2$ levels of the $3p^5 4s$ configuration). We compare our theoretical results with their experimental results and discuss the differences from the similar excitation to the $3p^5 4p$ levels from the same metastable states [9]. In the light of this work on argon, we feel that in xenon also the electron impact excitation of the ten higher-lying fine-structure levels of the $5p^5 7p$ configuration from the lowest metastable states (the $J = 0, 2$ levels of the $5p^5 6s$ configuration) possibly can contribute. This has to be tested and we are currently working on this aspect as well. In addition, as pointed out by the Hanscom group that the electron excitation of Xe^+ ion can influence the results of CRM model, we would therefore, like to test this as well. Currently, we are also planning to extend our RDW calculations to the excitation of Xe^+ ions which will be our future work.

8. References

1 G. F. Karabadzhak , Y. Chiu and R. A. Dressler, J. Appl. Phys., **99** (2006) 113305.

2 R. O. Jung, J. B. Boffard, L. W. Anderson and C. C. Lin, Phys. Rev. A, **72** (2005) 022723.

3 J. B. Boffard, C. C. Lin and C. A. Dejoseph Jr, J. Phys. D: Appl. Phys., **37** (2004) R-143.

4 Y. Chiu, B. L. Austin, S. Williams, R. A. Dressler and G. F. Karabadzhak, J. Appl. Phys., **99** (2006) 113304.

5 http://physics.nist.gov/PhysRefData/ASD/index.html

6 C.M. Maloney, J.L. Peacher, K. Bartschat and D.H. Madison, Phys. Rev. A, **61** (2000) 022701.

7 R. Srivastava, A. D. Stauffer and Lalita Sharma, Phys. Rev. A, **74** (2006) 012715.

8 R. O. Jung J. B. Boffard, L; W; Anderson and C. C. Lin., Phys. Rev. A **75**, (2007) 052707.

9 Lalita Sharma, R. Srivastava and A. D. Stauffer, Phys. Rev. A (in Press).

9. List of Publications

1. "Excitation of the metastable states of the noble gases", (R. Srivastava, A. D. Stauffer and Lalita Sharma), Phys. Rev. A **74** (2006) 012715.
2. "Excitation of the $3p^5 5p$ levels of Argon from the $3p^5 4s$ metastable levels", (Lalita Sharma, R. Srivastava and A. D. Stauffer), Phys. Rev. A (in Press).
3. "Excitation of the metastable states of argon", (Lalita Sharma, Rajesh Srivastava and A. D. Stauffer), Journal of Physics Conference Series (in Press).
4. "Excitation of the metastable states of the noble gases", (Lalita Sharma, Rajesh Srivastava and A. D. Stauffer), 7th Asian International Seminar on Atomic and Molecular Physics, 4th -7th December, 2006, IIT Madras, Chennai.
5. "Electron impact excitation of the initially excited atoms: A fully relativistic approach", (Rajesh Srivastava, Lalita Sharma and A.D. Stauffer), 9th European Conference on Atoms, Molecules & Photons, 6th – 11th May 2007, Heraklion, Greece.
6. "Excitation from the metastable states of inert gases", (Rajesh Srivastava, Lalita Sharma and A.D. Stauffer), 25th International Conference on Photonic, Electronic and Atomic Collisions (ICPEAC-XXV), Freiburg (Germany), July 25-31, 2007 (Accepted)
7. "Excitation from the ground states of inert gases", (Lalita Sharma, Rajesh Srivastava and A. D. Stauffer), 25th International Conference on Photonic, Electronic and Atomic Collisions (ICPEAC-XXV), Freiburg (Germany), July 25-31, 2007 (Accepted)
8. "Excitation of the $3p^5 5p$ levels of Argon from the $3p^5 4s$ metastable levels", (Rajesh Srivastava, Lalita Sharma and A.D. Stauffer), Gaseous Electronic Conference-2007, Arlington VA, October 2 -5, 2007, (Submitted)
9. "Passive optical diagnostic of electric propulsion Xe plasma: the role of metastable atoms", (R. A. Dressler, Y. Chiu, Lalita Sharma, R. Srivastava and G. Karabadzhak), Gaseous Electronic Conference-2007, Arlington VA, October 2 -5, 2007, (Submitted)